Published in final edited form as:
Dev Cell. 2008 July ; 15(1): 74–86. doi:10.1016/j.devcel.2008.05.005.

Neuraminidase 1 is a Negative Regulator of Lysosomal Exocytosis

Gouri Yogalingam[1,2,3], **Erik J. Bonten**[1,2], **Diantha van de Vlekkert**[1], **Huimin Hu**[1], **Simon Moshiach**[4], **Samuel A. Connell**[4], and **Alessandra d'Azzo**[1,*]

1*Department of Genetics and Tumor Cell Biology, St. Jude Children's Research Hospital, Memphis, TN 381052794, USA*

4*Cell and Tissue Imaging Shared Resource, St. Jude Children's Research Hospital, Memphis, TN 381052794, USA*

SUMMARY

Lysosomal exocytosis is a Ca^{2+}-regulated mechanism that involves proteins responsible for cytoskeletal attachment and fusion of lysosomes with the plasma membrane. However, whether luminal lysosomal enzymes contribute to this process remains unknown. Here we show that neuraminidase Neu1 negatively regulates lysosomal exocytosis in hematopoietic cells by processing the sialic acids on the lysosomal membrane protein Lamp-1. In macrophages from Neu1-deficient mice, a model of the disease sialidosis, and in patients' fibroblasts, oversialylated Lamp-1 enhances lysosomal exocytosis. Silencing of Lamp-1 reverts this phenotype by interfering with the docking of lysosomes at the plasma membrane. In *Neu1*$^{-/-}$ mice the excessive exocytosis of serine proteases in the bone niche leads to inactivation of extracellular serpins, premature degradation of VCAM-1, and loss of bone marrow retention. Our findings uncover an unexpected mechanism influencing lysosomal exocytosis and argue that exacerbations of this process form the basis for certain genetic diseases.

INTRODUCTION

Conventionally lysosomes have been viewed as the final stage in the degradation or recycling of endocytic or autophagocytic macromolecules by specialized hydrolases (Kornfeld and Mellman, 1989). Their importance in normal cell homeostasis is emphasized by the many genetic defects that hamper lysosomal degradation and cause disease (Sandhoff et al., 2001). In addition to their general digestive capacity, lysosomes serve a multitude of basic cellular functions, including downregulation of membrane receptors, disruption of internalized pathogens and processing of MHC class II antigens (Li et al., 2005; Ni et al., 2006; Seto et al., 2002). Lysosomes are also actively involved in specialized, regulated functions that reflect the physiological properties of individual cell types. For example, secretory lysosomes, which are present in melanocytes and hematopoietic cells, contain in addition to their usual composite of lysosomal hydrolases, unique secretory proteins that require routing through an acidic compartment prior to secretion. These specialized lysosomes expel their content by lysosomal exocytosis, a regulated process that entails recruitment/docking of lysosomes to the plasma membrane (PM), followed by the Ca^{2+}-dependent fusion of the lysosomal membrane (LM) with the PM, so that the luminal side of the LM becomes exposed extracellularly (Andrews, 2000; Bossi et al., 2005; Bossi and Griffiths, 2005).

[2]These authors contributed equally to this work.
[3]Present address: Department of Pharmacology and Cancer Biology, Duke University Medical Center, Durham, NC 27710, USA
[*]Correspondence: sandra.dazzo@stjude.org

Exocytosis of lysosomes has now emerged as a fundamental mechanism in physiologic and pathologic processes such as replenishment of the PM in macrophages, repair of damaged PM, and the removal of pathogenic bacteria or the release of human immunodeficiency virus from infected cells (Huynh et al., 2004; Jaiswal et al., 2002; McNeil and Steinhardt, 2003; Reddy et al., 2001; Roy et al., 2004). Numerous gene defects are known to be associated with impaired exocytosis of secretory lysosomes in cytotoxic T lymphocytes, platelets, and melanocytes; these diseases share the common clinical features of immunodeficiency, bleeding disorders, and albinism (Stinchcombe et al., 2004). Characterization of these genetic lesions has identified proteins required for the movement of lysosomes along the microtubule network, fusion with the PM, and ultimately exocytosis of their luminal content (Bossi et al., 2005; Bossi and Griffiths, 2005). However, whether lysosomal luminal proteins participate in this process is not yet known.

Recent studies suggest that components of the LM itself play a pivotal role in exocytosis. The ubiquitously expressed lysosomal synaptotagmin VII (Syt VII) is a Ca^{2+} sensor that is anchored to the LM by a single transmembrane domain, while the majority of the protein is exposed to the cytosol. Syt VII cooperates with V- and T-soluble N-ethylmaleimide sensitive factor attachment receptor (SNARE) proteins in promoting the fusion of the LM with the PM (Andrews and Chakrabarti, 2005; Gerasimenko et al., 2001; Kima et al., 2000; Martinez et al., 2000). Deficiency of Syt VII in mice hampers lysosomal exocytosis, leading to decreased LM-mediated PM repair and the onset of autoimmune myositis (Chakrabarti et al., 2003).

LAMP-1 is an important structural constituent of lysosomes localized abundantly in the limiting membrane of the organelle and sparsely at the PM, unless cells undergo exocytosis (Furuno et al., 1989; Lippincott-Schwartz and Fambrough, 1987). In contrast to Syt VII, its primary structure consists of a highly glycosylated and sialylated N-terminal portion oriented towards the lumen, a short cytoplasmic tail, and a single transmembrane domain (Eskelinen et al., 2003). LAMP-1 has been implicated in the process of lysosomal exocytosis, because its overexpression was shown to increase its abundance at the PM and to enhance lysosomal exocytosis of β-hexosaminidase (Kima et al., 2000). However, the physiological relevance of this effect is unclear, as Lamp-1 mutant mice appear to have a very mild phenotype (Andrejewski et al., 1999).

Most hydrolases deficient in lysosomal storage diseases (LSDs) are carbohydrate-cleaving exoglycosidases. Among them, N-acetyl-α-neuraminidase (NEU1, sialidase) initiates the catabolism of sialo-glycoconjugates by removing their terminal sialic acid residues (Bonten et al., 1996; Rottier et al., 1998). *NEU1* gene mutations in humans cause sialidosis, a clinically-heterogeneous autosomal recessive LSD that targets primarily the reticuloendothelial system. Sialidosis patients have a severe systemic disease, which includes hepatosplenomegaly and involvement of the nervous system (Thomas, 2001). *Neu1* knockout (KO) mice closely mimic the human condition, and develop a pronounced, age-dependent splenomegaly characterized by elevated numbers of hematopoietic progenitors, consistent with splenic extramedullary hematopoiesis (EMH) (de Geest et al., 2002).

Although much is known about the lysosomal enzymes that are deficient in LSDs, there is a lesser understanding of the range of natural substrates they target in vivo and how accumulation or lack of processing of such substrates may contribute to the pathogenesis of each disorder. Here, we have identified LAMP-1 as a target substrate of NEU1. We found that in *Neu1*$^{-/-}$ hematopoietic cells an oversialylated form of Lamp-1 accumulates at the PM, and is associated with enhanced lysosomal exocytosis of catalytically active hydrolases. The resulting increase in extracellular proteolytic activity leads to premature degradation of vascular cell adhesion molecule-1 (VCAM-1), which is crucial for bone marrow (BM) retention in the bone niche.

Our results identify NEU1 as a negative regulator of lysosomal exocytosis, and link an exacerbation of this process to a disease condition.

RESULTS

Extracellular Clade-A Serpins Are Downregulated in the *Neu1*$^{-/-}$ Bone Niche

To explain the EMH phenotype characteristic of *Neu1*$^{-/-}$ mice (de Geest et al., 2002) we argued that a loss of Neu1 activity could lead to changes in the BM microenvironment, and, in turn, to loss of BM retention and/or homing. This became evident after a series of bone marrow transplantations (BMTs), in which Neu1-expressing transgenic BM was transplanted into sub-lethally irradiated *Neu1*$^{-/-}$ mice. Treated mice showed consistently successful short-term engraftment (10 days post BMT), but failed long-term engraftment (n=25; >16 days post BMT), whereas all control BMTs into wild-type (WT) mice showed sustained short- and long-term engraftment (n=8) (not shown). These results demonstrated a defect in bone marrow retention rather than in BM homing.

We reasoned that EMH and lack of BM engraftment in *Neu1*$^{-/-}$ mice could have a common determinant, namely impaired processing of sialic acid on glycans of yet unknown Neu1 targets that would affect their biochemical properties. In fact, using a sialic acid detection assay, we showed that *Neu1*$^{-/-}$ total BM extracts contained high levels of sialylated proteins compared to WT (Supplemental Figure S1). We next performed comparative proteomic analyses of the BM extracellular fluid (BMEF) from *Neu1*$^{-/-}$ and *Neu1*$^{+/+}$ mice to identify proteins that were deregulated by the loss of Neu1. Total protein preparations from the two BMEFs were analyzed on 2-dimensional (2D) SDS gels and selected single-protein spots identified by MALDI-TOF (Figure 1A). The most overt difference was a reduction in the *Neu1*$^{-/-}$ BMEF of two clusters of uncleaved, clade A serine protease inhibitors, serpina1 and serpina3 (Figure 1A). Serpins are present extracellularly in two forms, an uncleaved inert form, and a cleaved activated form. Specific serine proteases cleave the reactive center loop of serpins, which allows them to covalently bind and inactivate these proteases; the resulting serpin-protease complexes (SECs) are rapidly cleared from the body (Winkler et al., 2005). Discrete spots on the 2D gels represented both the uncleaved (closed ovals) and cleaved (dashed ovals) serpins, as well as different variants derived from multiple *serpina1* and *serpina3* genes (Borriello and Krauter, 1991; Forsyth et al., 2003). Both inhibitors were readily detected by immunohistochemistry (IHC) in the extracellular matrix (ECM) of WT bone sections, where they normally bind to specific glycosaminoglycans (Patston et al., 2004); but they were drastically reduced in KO bone sections (Figure 1B). Western blot analysis of *Neu1*$^{+/+}$ and *Neu1*$^{-/-}$ BMEFs confirmed these results (Figure 1C). The decreased levels of uncleaved serpins in *Neu1*$^{-/-}$ BMEF were likely due to excessive processing of these proteins, because their mRNA levels were unchanged (not shown).

The physiological excess of clade A serpins in plasma and BMEF (Winkler et al., 2005) reflects their role in controlling the load of potentially harmful free serine proteases. We therefore asked whether the decreased levels of uncleaved serpins in *Neu1*$^{-/-}$ BMEF was due to an abnormal increase of serine proteases. To test this hypothesis, we incubated recombinant human SERPINA1 (rSERPINA1) with *Neu1*$^{-/-}$ BMEF, which indeed resulted in the *in vitro* formation of SECs of higher molecular weight (MW) than the unbound species; SECs were not formed with WT BMEF (Figure 1D).

Increased Levels of Neutrophil Serine Proteases in *Neu1*$^{-/-}$ BMEF

A crucial process for the maintenance of BM homeostasis is the regulated exocytosis of serine proteases, such as neutrophil elastase (NE) and cathepsin G (CG), by neutrophils that degranulate their secondary granules (secretory lysosomes) into the BM-ECM (Levesque et

al., 2001). We therefore tested the expression pattern of these proteases by IHC of bone sections. A drastically reduced intracellular staining of NE and CG was observed in *Neu1*$^{-/-}$ sections compared to WT (Figure 1E). Conversely, elevated amounts of these proteases were detected in the *Neu1*$^{-/-}$ BMEF (Figure 1F), indicating abnormal extracellular release of these proteases.

To validate this observation, we performed casein zymography that detected additional serine proteases in *Neu1*$^{-/-}$ BMEF not present in the WT sample (Figure 1G). One of these was unequivocally identified as CG by using a selective CG inhibitor that completely abolished a low MW band present only in *Neu1*$^{-/-}$ BMEF (Figure 1G, yellow diamond). We could not determine the exact identity of the remaining proteases in the *Neu1*$^{-/-}$ BMEF, albeit their activities were inhibited upon incubation with a selective elastase inhibitor, suggesting that they might have overlapping elastase activity (Figure 1G, blue diamond).

High Elastase Activity in *Neu1*$^{-/-}$ BMEF Degrades VCAM-1 and Causes Loss of Retention of BM Progenitors in the Bone Niche

Based on the above results, we next determined the relative amount of endogenous VCAM-1 in *Neu1*$^{-/-}$ BM stromal cells (BMSCs). BM progenitor cells are retained in the bone niche by chemotactic interactions between CXCL-12 and CXCR-4, and adhesive interactions between the β-integrin VLA-4 and VCAM-1. We found no differences in the levels of CXCR-4 and VLA-4 protein between KO and WT samples (data not shown). We, therefore, focused on VCAM-1 because it is expressed on the surface of BMSCs, is crucial for the homing and retention of BM cells in the bone niche, and is proteolytically regulated by serine proteases (Levesque et al., 2001). VCAM-1 protein levels were abnormally low in *Neu1*$^{-/-}$ BMSC extracts compared to WT (Figure 2A). This was occurring post-translationally, because *VCAM-1* mRNA levels were identical in KO and WT BMSCs (not shown). Moreover, in total BM isolated from *Neu1*$^{-/-}$ mice of different ages the amount of VCAM-1 decreased progressively as the animals aged (Figure 2A). These data were validated by FACS analyses of BM that detected a lower number of VCAM-1^{+} cells in the *Neu1*$^{-/-}$ sample compared to WT (Figure 2B), and by IHC of bone sections that showed reduced VCAM-1 levels in the *Neu1*$^{-/-}$ stromal cells lining the bone cavity (Figure 2C, arrows).

To prove that the decrease in VCAM-1 in KO cells was caused by enhanced proteolytic activity extracellularly, we incubated recombinant human VCAM-1 (rVCAM-1) with *Neu1*$^{-/-}$ or *Neu1*$^{+/+}$ BMEFs and only observed the generation of numerous low MW digested VCAM-1 products with *Neu1*$^{-/-}$ BMEF (Figure 2D, left panel). Proteolysis of rVCAM-1 was prevented by an elastase inhibitor (Figure 3D, right panel), confirming the presence of high elastase activity in the KO BMEF. Furthermore, incubation of cultured BMSCs with *Neu1*$^{-/-}$ BMEF, but not with WT BMEF, resulted in the cleavage of VCAM-1. This cleavage was blocked by the serine protease inhibitor PMSF (Figure 2E). From these data we inferred that the abnormally high serine protease activity towards VCAM-1 in the *Neu1*$^{-/-}$ BMEF could hamper the capacity of the BMSCs to retain hematopoietic progenitor cells (HPCs) in the bone niche.

We verified this hypothesis by performing cell adhesion assays between cultured WT BMSCs and purified c-Kit^{+}/Sca1^{+}/Lin^{-} HPCs (Levesque et al., 2001). To mimic the BM microenvironment of Neu1-deficient mice we incubated WT BMSCs with increasing concentrations of *Neu1*$^{-/-}$ BMEF. This gradually prevented the adherence of HPCs to the BMSC layer (Figure 2F). In contrast, *Neu1*$^{+/+}$ BMEF had no such effect. In agreement with these results, we observed an increased mobilization of HPCs into the peripheral blood of *Neu1*$^{-/-}$ mice compared to WT mice, which was accompanied by a reduction in the number of these cells in the *Neu1*$^{-/-}$ BM (Figure 2G). Together these findings may explain the time-dependent loss of BM retention in the bone niche of KO mice and provide a rationale for the occurrence of EMH in this mouse model.

Neu1$^{-/-}$ Mice Have Enhanced Lysosomal Exocytosis in the Bone Niche

We reasoned that the excess of proteolytically active serine proteases in the BMEF of KO mice (Figure 1) could only be the result of increased lysosomal exocytosis of BM cells, because these enzymes are normally synthesized as zymogens and converted to their mature, active forms in the endo/lysosomal compartment (Kominami et al., 1988). We therefore analyzed by FACS the percentage of *Neu1*$^{-/-}$ and *Neu1*$^{+/+}$ BM cells with Lamp-1 at their PM, a parameter used to distinguish cells engaged in lysosomal exocytosis. A clear increase in the percentage of Lamp-1^{+} cells was detected in the *Neu1*$^{-/-}$ total BM compared to WT (Figure 3A). The difference in number of Lamp-1^{+} cells between WT and KO was even greater in sorted neutrophils (60 fold increase in the KO sample)(Figure 3B). These cells are the main source of extracellular serine protease activities (NE and CG) in the bone niche, which they release via lysosomal exocytosis of Lamp-1^{+} secretory granules (Dahlgren et al., 1995). Hence, the increased number in the *Neu1*$^{-/-}$ BM of neutrophils with Lamp-1 at their PM likely accounted for the increased levels of these enzymes in the BMEF.

Because cell-surface expression of Lamp-1 by itself was not a quantitative indicator of lysosomal exocytosis, as a functional read-out of this process we measured the enzyme activities of several other lysosomal cathepsins and glycosidases in BMEF samples. These enzymes are stored in Lamp-1^{+} conventional lysosomes of most BM cells, and are normally not present at high levels extracellularly. However, these enzyme activities were found to be 4- to 6-fold higher in *Neu1*$^{-/-}$ BMEF than in the WT BMEF (Figure 3C). By contrast, the same enzyme activities measured in the BMEF from β-galactosidase-deficient (*β-gal-KO*) mice, a model of the LSD GM1-gangliosidosis (Hahn et al., 1997), were normal, indicating that the exocytic release of active lysosomal hydrolases was intrinsic to the Neu1 deficiency and not a feature shared by other LSDs (Figure 3C).

Lamp-1 is a Natural Substrate of Neu1

To reconcile the loss of Neu1 activity with the excessive lysosomal exocytosis of hematopoietic cells, we postulated a role for Neu1 in the processing of glycans on lysosomal proteins that have been implicated in the exocytic process, thereby changing their properties. Using primary macrophage cultures (Bonten et al., 2004) as an in vitro model of exocytic cells, we first determined that Neu1 was not involved in the processing of two LM-anchored proteins, Syt VII and VAMP7, which participate in the LM-PM fusion (Andrews and Chakrabarti, 2005; Kima et al., 2000). On immunoblots these proteins showed an identical mobility pattern and expression level in KO and WT macrophages (Supplemental Figure S2). Also the T-SNAREs, syntaxin4 and SNAP23 which are anchored to the PM (Stinchcombe et al., 2004) were unaltered (Figure S2). Thus, Neu1 deficiency does not affect proteins that are part of the fusion machinery.

In contrast, immunoblots of total macrophage lysates probed with Lamp-1 antibodies against either the C-terminal cytosolic domain (L1418) or the glycosylated luminal domain (1D4B), identified a Lamp-1 protein in *Neu1*$^{-/-}$ cells that was increased in amount and MW with respect to WT Lamp-1 (Figure 4A). In vitro enzymatic removal of all N- and O-glycans released a core-Lamp-1 protein of ~40-kDa from both KO and WT macrophage lysates, indicating that the differential mobility of Lamp-1 in absence of Neu1 was solely due to its glycan composition (Supplemental Figure S3A). We further demonstrated that the abnormal MW of Lamp-1 (~140 kDa) was normalized to ~125 kDa after reconstitution of Neu1 activity in deficient cells that had taken up a recombinant enzyme (rBV-Neu1; Figure 4B). Thus, the higher Lamp-1 MW in KO cells was caused by oversialylation of the protein. No relevant differences were observed in the relative sizes and amounts of 2 other LM glycoproteins, Lamp-2 and Limp-1 (Figure S3C).

The increased Lamp-1 level in deficient cells was not due to enhanced transcription (Figure S3B). Therefore, we performed a pulse-chase experiment to assess the processing and turnover of Lamp-1 in KO and WT macrophages (Figure 4C). Immunoprecipitation of radiolabelled proteins with L1418 antibody demonstrated that in WT cells a 140 kDa newly synthesized Lamp-1 was converted into a 125 kDa species over a <48 hr chase period, and had a half-life of ~20 hr (Figure 4C). Instead, in KO macrophages only a partially processed Lamp-1 had a half-life of >96 hr (Figure 4C). Remarkably, the processing and turnover of Lamp-2 was unaltered in these cells (Figure 4D). These results indicate that Lamp-1 is a substrate of Neu1 and that the loss of this enzyme preferentially decreases the turnover rate of Lamp-1.

To further investigate the effect of Neu1 on the sialylation and stability of Lamp-1, we cultured *Neu1*$^{-/-}$ macrophages in the presence of rBV-Neu1 and then chased the internalized enzyme in Neu1-free medium. Exposure to rBV-Neu1 reduced the MW of Lamp-1, and its amount was less than 10% of that in untreated KO macrophages (Figure 4E, t=0). During the first 4 hr of the chase the levels of Lamp-1 remained low, in agreement with the high amount of Neu1. In contrast, during prolonged chase periods, the amount of Neu1 decreased drastically, which reversed the amount and size of Lamp-1 to those detected in untreated KO macrophages (Figure 4E, t=24-28h). Thus, Neu1 is responsible for the processing of the sialic acid residues of Lamp-1, which in turn increases its turnover.

Localization of sialylated Lamp-1 at the PM of *Neu1*$^{-/-}$ Cells Correlates with Increased Lysosomal Exocytosis

To ascertain whether oversialylation affected the abundance and subcellular distribution of Lamp-1, *Neu1*$^{-/-}$ cells were probed with either the 1D4B (luminal domain) or L1418 (cytosolic tail) Lamp-1 antibody and examined by immunofluorescence and laser scanning confocal microscopy (LSCM). Under conditions that permeabilized the PM, the intracellular pool of Lamp-1^{+} lysosomes in KO macrophages appeared clustered and often juxtaposed to the cell surface (Figure 5A, and Movie S1), while in WT cells a typical punctated Lamp-1 distribution was seen throughout the cytosol (Figure 5A and Movie S2). In contrast, under conditions that did not permeabilize the PM, Lamp-1 was present abundantly at the cell surface of KO cells but hardly visible at the surface of WT macrophages (Figure 5A, and Movies S3 and S4). The differential localization of Lamp-1 in *Neu1*$^{-/-}$ cells was specifically due to loss of Neu1 activity rather than mere expansion of the lysosomal compartment, because *β-gal*$^{-/-}$ macrophages showed a normal Lamp-1 distribution (Supplemental Figure S4).

We postulated that the preferential redistribution of Lamp-1 at the PM of KO macrophages could be a direct consequence of increased lysosomal exocytosis in these cells. Given that lysosomal exocytosis depends on the rapid influx of Ca^{2+} at the PM, we asked whether the localization of Lamp-1 at the PM of Neu1 deficient cells was Ca^{2+}-dependent and whether this was accompanied by excessive lysosomal exocytosis. Similarly to what was observed in neutrophils, FACS analysis with the 1D4B antibody showed a higher percentage of KO macrophages with Lamp-1 at their cell surface compared to WT cells (Figure 5B). Restoring Neu1 activity in deficient cells by uptake of rBV-Neu1 reversed the cell surface localization of Lamp-1 (Figure 5B). Most importantly, WT and KO macrophages that were maintained in Ca^{2+}-free medium (+EGTA) for more than 2 hr prior to FACS analysis were nearly devoid of Lamp-1 at the PM (Figure 5B). Thus, the localization of Lamp-1 at cell surface of macrophages depends on the influx of Ca^{2+}.

We further tested whether induction of lysosomal exocytosis would differentially affect the PM localization of Lamp-1 in KO versus WT macrophages. For this purpose cells were treated with calcimycin, a Ca^{2+} ionophore that promotes the rapid influx of Ca^{2+} at the cell surface and, in turn, the fusion of already docked lysosomes with the PM (Jaiswal et al., 2002). After induction, cells were cultured in Ca^{2+}-free medium for up to 1 hr to prevent further fusion of

lysosomes with the PM (Figure 5C). We found that purified preparations of the PM from calcimycin-treated *Neu1*$^{-/-}$ macrophages contained high quantities of a Lamp-1 species of higher MW than did similar preparations from treated WT cells (Figure 5C). The pool of PM-localized Lamp-1 in KO cells remained unchanged for up to 1 hr upon withdrawal of Ca^{2+} from the medium; in contrast, in WT cells the majority of Lamp-1 was recovered intracellularly at all time points (Figure 5C). These results suggest that in KO cells a larger number of lysosomes than in WT cells were docked at the PM and underwent lysosomal exocytosis exposing Lamp-1 at the cell surface.

Finally, purification of PM fractions with a sialic acid-specific lectin demonstrated that Lamp-1 from both KO and WT cells was sialylated at the PM, albeit the MW of KO-Lamp-1 was higher than that of WT-Lamp-1 because of differential sialic acid content (Figure 5D). We also measured increased extracellular activity of β-hexosaminidase (β-hex) and α-mannosidase (α-man) in the medium of *Neu1*$^{-/-}$ cells, which confirmed their enhanced lysosomal exocytosis (Figure 5E).

Neu1 Activity in Sialidosis Fibroblasts Inversely Correlates with LAMP-1 levels at the PM and Lysosomal Exocytosis

We next tested whether the phenotypic abnormalities seen in Neu1-deficient murine macrophages were reproduced in fibroblasts from sialidosis patients (Bonten et al., 2000). Two of these patients presented at birth with the congenital early onset form of the disease (Type II) and carried *NEU1* mutations that completely eliminated NEU1 activity; the third was a late onset patient with residual lysosomal NEU1 activity and an attenuated form of sialidosis (Type I). All of the tested sialidosis fibroblasts had increased levels of LAMP-1 in the total cell lysate compared to the normal fibroblasts (Figure 5F). LAMP-1 was nearly absent in purified PM fractions isolated from normal fibroblasts, reflecting the preferential LM localization of the protein in these cells (Figure 5F). In contrast, PM fractions from sialidosis fibroblasts showed a clear correlation between disease severity and the levels of cell surface LAMP-1 (Figure 5F). The increased levels of LAMP-1 at the PM of the type II sialidosis fibroblasts were accompanied by higher extracellular activity of α-man, indicative of increased exocytosis (Figure 5G). The relatively low levels of LM-localized LAMP-1 in the type II sialidosis fibroblasts reflected a clear redistribution of this protein from the LM to the PM (Figure 5F). In contrast, the type I sialidosis fibroblasts showed a near normal distribution of LAMP-1 (Figure 5F), and in turn no significant increase in lysosomal exocytosis (Figure 5G). Based on these results, we postulate that also in non-secretory cells a complete lack of NEU1 activity results in the redistribution of LAMP-1 to the PM and the aberrant induction of lysosomal exocytosis.

Neu1$^{-/-}$ Macrophages Form Clusters of Lysosomes in the Proximity of the PM

It has been shown that lysosomes that are destined to undergo lysosomal exocytosis are pre-docked at the PM, a process that is independent of Ca^{2+} influx (Jaiswal et al., 2002). We reasoned that accumulation of Lamp-1 at the cell surface of Neu1-deficient macrophages may not only reflect an increase in lysosomal exocytosis, but also be indicative of a higher number of pre-docked lysosomes near the PM. To test this hypothesis we used total internal reflection microscopy (TIRFM), which allows the visualization of fluorescently labeled organelles in the evanescent field near the cell surface (Axelrod, 1981; Jaiswal et al., 2002). The lysosomes of KO and WT macrophages were labeled with Lysotracker to monitor the number of PM-proximal lysosomes present in the TIRF field. *β-gal*$^{-/-}$ macrophages were included in this experiment as a control. Lysotracker^{+} objects were counted in multiple KO and WT TIRF images, and compared to those present in the epifluorescent field (Figure 6A). All macrophages had numerous small lysosomes in the TIRF-field, but only the *Neu1*$^{-/-}$ macrophages contained large lysotracker^{+} objects (>1 μm) intensely fluorescent (Figure 6A and B). The mean size of

these objects in the *Neu1*$^{-/-}$ cells was approximately 3-fold larger than that in WT and *β-gal*$^{-/-}$ macrophages (Figure 6C). Their irregular shape was suggestive of clusters or aggregates of lysosomes rather than individual enlarged lysosomes (Figure 6A); moreover, both their shape and fluorescence intensity fluctuated in the TIRF field. This fluctuation in signal was probably caused by the continuous addition and release of lysosomes to and from these clusters, many of which likely fusing with the PM. We propose that these clusters in *Neu1*$^{-/-}$ cells represent dynamic 'lysosome docking stations' from which lysosomal exocytosis occurs.

In agreement with the TIRFM data, electron microscopy (EM) of cultured *Neu1*$^{-/-}$ cells showed the majority of lysosomes decorating the PM (Figure 6D), middle and left panels). The right panel gives an example of a lysosome in a KO cell that has breached the PM and is undergoing exocytosis (arrows).

Lamp-1 Regulates the Extent of Lysosomal Exocytosis

Given the direct correlation between increased Lamp-1 at the PM and enhanced lysosomal exocytosis, we asked whether overexpression of Lamp-1 in WT macrophages would induce a similar phenotype, albeit without the additional effect of oversialylation occurring in Neu1-deficient cells. Western blot analysis of WT cells overexpressing Lamp-1 showed increased levels of the protein that was paralleled by an increment of α-man activity in the medium (Figure 7A and B). Nonetheless this activity was considerably lower than that measured in the medium of KO cells; therefore, overexpression of wild-type Lamp-1 did not fully recapitulate the effects of hypersialylated Lamp-1 on lysosomal exocytosis.

To further support this point, we assessed whether siRNA silencing of Lamp1 in *Neu1*$^{-/-}$ and *Neu1*$^{+/+}$ macrophages would hamper lysosomal exocytosis. This experiment was performed with or without addition in the medium of calcimycin. As seen earlier, KO macrophages were especially responsive to calcimycin treatment, which substantially increased the level of exocytosed β-hex; whereas this drug had only a marginal effect on WT macrophages (Figure 7D). Again, these results imply that Neu1-deficient macrophages contain a larger population of lysosomes docked at the PM and poised for exocytosis. Transfection of both KO and WT cells with *Lamp-1* siRNA effectively reduced Lamp-1 protein levels (Figure 7C). Silencing of *Lamp-1* mRNA was accompanied by a dramatic inhibition of lysosomal exocytosis, particularly in deficient cells, reducing extracellular β-hex activity to levels similar to those measured in the medium of WT cells (Figure 7D). The β-hex activity did not increase when calcimycin was added to siRNA-transfected WT and Neu1-deficient macrophages (Figure 7D).

Finally, we monitored by LSCM the distribution of Lysotracker-labelled lysosomes in live cells after silencing of Lamp-1. Contrary to mock-transfected WT macrophages, which had a relatively random distribution of lysosomes (Figure 7E and Movie S5), mock-transfected KO macrophages showed clusters of lysosomes (Figure 7E; arrow). Z-stacks imaging of these clusters confirmed that they were located at or near the cell surface (Movie S6). Silencing of Lamp-1 completely reversed the formation of lysosome clusters in *Neu1*$^{-/-}$ macrophages (Figure 7E and Movie S7-S8).

Combined, these results suggest that Lamp-1 promotes the formation of clusters of lysosomes near the cell surface of *Neu1*$^{-/-}$ macrophages, which are likely responsible for the increase in exocytosis.

DISCUSSION

In this study we identify an unexpected function of Neu1 as a negative regulator of Lamp-1, a structural component of the lysosomal membrane. Together with other LM proteins, including the structurally similar LAMP-2, LAMP-1 was thought to merely maintain membrane integrity

against the harsh lysosomal environment, owing to its abundant sugar content (Kundra and Kornfeld, 1999). KO mice for the individual Lamps have suggested partial redundancy between the two proteins (Andrejewski et al., 1999; Tanaka et al., 2000). LAMP-2 has since been recognized as a multitask protein involved in macroautophagy, chaperone-mediated autophagy and lysosomal biogenesis, and deficiency of one of its isoforms in humans causes Danon disease (Cuervo et al., 2003; Eskelinen et al., 2003; Oakes et al., 2005). On the other hand, LAMP-1 has been implicated in lysosomal exocytosis (Kima et al., 2000; Reddy et al., 2001). More recently, both Lamp-1 and Lamp-2 were shown to be involved in the movement of lysosomes along microtubules, because double-deficient cells have impaired organelle motility and a defect in the fusion of phagosomes with lysosomes (Huynh et al., 2007). Therefore, it is clear that these proteins exert specialized and regulated functions in different cells.

Our current findings support this notion and put forward a mechanism of regulation of the intracellular trafficking of Lamp-1 that hinges on its sialic acid cleavage by Neu1. By controlling the sialic acid content of the luminal domain of Lamp-1, Neu1 determines its turnover rate and subcellular distribution, and, in turn, impacts on the physiological process of lysosomal exocytosis. In *Neu1*$^{-/-}$ BM-derived macrophages the loss of Neu1 results in hypersialylated Lamp-1, which has a longer half-life and is preferentially accumulated at the PM. We provide evidence that these features of Lamp-1 promote excessive lysosomal exocytosis of serine proteases in the bone niche of affected mice and consequent loss of BM retention.

Two events must occur with precision for lysosomes to undergo exocytosis, both of which may be differentially regulated in different cell types: the recruitment/docking of lysosomes to the PM, which is a Ca^{2+}-independent process, and the actual fusion of the LM with the PM, which is strictly dependent on Ca^{2+} influx (Jaiswal et al., 2002). We found no evidence that the absence of Neu1 has any effects on the fusion of lysosomes with the PM, because the MW or stability of T- and V-SNAREs, and Syt VII, which are involved in the LM-PM fusion during lysosomal exocytosis (Shen et al., 2005; Tucker et al., 2004;Rizo et al., 2006), remain unaltered in KO cells. However, inhibition of Lamp-1 expression effectively blocks exocytosis in *Neu1*$^{-/-}$ macrophages and alters lysosome distribution, directly implicating Lamp-1 in the recruitment and/or docking of lysosomes to the PM. Several proteins, including Rab GTPases and motor myosins, are needed for the attachment of lysosomes to microtubules and subsequent delivery to the actin cytoskeleton at the periphery of the cell (Bossi et al., 2005). We can speculate that the highly conserved cytosolic tail of Lamp-1 interacts with components of this transport machinery. However, as is the case for many receptor-ligand interactions, by controlling the sialic acid content of the Lamp-1 luminal domain, Neu1 may actually alter the charge/conformation of the cytosolic tail of the protein at the other side of the LM and, thereby, change its binding affinity towards its interacting partners. On the other hand, the extent by which Lamp-1 is involved in lysosomal exocytosis could simply be dictated by its overall quantity. In the absence of Neu1 a larger pool of a long-lived Lamp-1 may be available for engaging lysosomes in exocytosis. Our findings support both concepts because i) those cells with no residual NEU1 activity have the highest levels of LAMP-1 at the PM (Type II sialidosis); ii) increasing Lamp-1 expression in WT cells failed to fully recapitulate the same extent of lysosomal exocytosis observed in *Neu1*$^{-/-}$ cells. Therefore, while in Neu1-deficient mice enhanced lysosomal exocytosis clearly plays a strong pathophysiological role, it remains to be determined whether Neu1-regulated processing of Lamp-1 significantly contributes to the physiological modes of exocytosis during normal development and homeostasis. It would be relevant to test this idea in *Lamp-1/Neu1* double KO mice. Unfortunately, both single mutant mice breed poorly (de Geest et al., 2002; P. Saftig, personal communication), and therefore this represents a long term project for the future.

We focused on understanding the consequences of increased lysosomal exocytosis in the bone niche in an attempt to characterize the molecular mechanism of EMH in sialidosis mice (de Geest et al., 2002). We found a dramatic inactivation of serpina1 and serpina3 in the *Neu1*$^{-/-}$ BMEF, coupled with mobilization of HPCs into the peripheral blood. Consequently, we detected a loss of intracellular staining of the neutrophil serine proteases NE and CG and corresponding increases of these proteins extracellularly, resulting in the degradation of VCAM-1 needed for the retention of HPCs. These findings agree with earlier studies that showed down-regulation of serpina1 and serpina3 upon massive release of neutrophil serine proteases following BM mobilization induced by G-CSF or chemotherapy (Winkler et al., 2005). Thus, a shift in the balance between serine proteases and serpins in the ECM of the *Neu1*$^{-/-}$ bone niche may contribute to the increased number of HPCs in the spleen of *Neu1*$^{-/-}$ mice, consistent with splenic EMH, and to the impaired long-term BM engraftment in sialidosis mice. Notably, patients with sialidosis exhibit a profound enlargement of the liver and spleen (Thomas, 2001), which could also be caused by NEU1-induced EMH.

In conclusion, this study introduces a mechanism for regulation of lysosomal exocytosis, which depends on the level of sialylation of Lamp-1 controlled by Neu1 and underscores the importance of this enzyme in lysosomal biogenesis and hematopoiesis in the bone niche (Figure 8). Moreover, to our knowledge, sialidosis is the only genetic disease known to date that is associated with increased lysosomal exocytosis, and it is likely that deregulation of this process underlies other phenotypic abnormalities in this complex multisystemic disease.

EXPERIMENTAL PROCEDURES

Animals

All procedures in mice were performed according to animal protocols approved by our Institutional Animal Care and Use Committee and NIH guidelines. *Neu1*$^{-/-}$ and *Neu1*$^{+/+}$ mice were bred into the FVB/NJ genetic background.

Cell Culture

Human skin fibroblasts from controls and sialidosis patients were cultured as described (Bonten et al., 2000). Primary macrophage and BMSC cultures were established from freshly isolated BM of WT or Neu1-deficient mice according to the procedure of (Sklar et al., 1985).

Antibodies, Recombinant Proteins and Protease Inhibitors

We used the following commercial antibodies: polyclonal anti-Lamp-1 raised against the C-terminal cytosolic peptide (Sigma; L1418); monoclonal anti-Lamp-1 against the luminal domain (clone 1D4B, Santa Cruz Biotechnology); polyclonal anti-Lamp-2 (Ipg96, Invitrogen); polyclonal anti-NE and -CG (Santa Cruz Biotechnology); polyclonal anti-SNAP23 (Santa Cruz Biotecnology); polyclonal anti-Syntaxin4 (Sigma); monoclonal anti-VAMP7 (Abcam); polyclonal Synaptotagmin VII (Synaptic Systems); polyclonal anti-actin (Cell Signaling); monoclonal anti-fibroblast surface protein (Novus Biologicals). Recombinant proteins, anti-SERPINA1, anti-SERPINA3, and anti-VCAM-1/CD106 were from R&D Systems. FITC-, CY3- and HRP-conjugated secondary antibodies were from Jackson Immuno Research. Polyclonal anti Neu1- and anti-CA antibodies have been previously described (Bonten et al., 2004). Elastase inhibitor III and CG inhibitor were from EMD Bioscience, and PMSF from Sigma.

IHC and Microscopy

IHC of tissue sections and immunofluorescence (IF) of permeabilized macrophages were performed as described (Bonten et al., 2004; de Geest et al., 2002). For IF of non-permeabilized

cells the fixation was done in ice-cold ultrapure paraformaldehyde (4%-w/v) and gluteraldehyde (5%-w/v). For lysotracker-fluorescence microscopy, macrophages were seeded in glass-bottom Fluorodishes (World Precision Instruments), and incubated for 30 min at 37° C in medium containing 200-nM Lysotracker (DND-99, Invitrogen). TIRFM of live lysotracker-labeled macrophages was performed with a Marianas imaging system (Intelligent Imaging Innovations/3i) consisting of a Carl Zeiss 200M motorized inverted microscope and TIRF illuminator (Carl Zeiss MicroImaging) and a DPSS 561 nm laser (Cobolt). Images were acquired with a Zeiss Alpha Plan-Fluar 100× 1.45 NA objective on a CoolSNAP HQ 2 CCD camera (Photometrics), using SlideBook 4.2 software (3i). LSCM on lysotracker-stained live cells was performed with a Nikon TE2000-E inverted microscope equipped with a C1Si confocal system, an argon ion laser at 488nm and a 561 nm DPSS laser (Melles Griot). Images were taken using a Nikon Plan Apochromat 60X 1.4 NA objective. LSCM on fixed tissues was performed with a Zeiss Axioplan 2 upright microscope equipped with an LSM 510 NLO confocal system (Carl Zeiss MicroImaging), a Mira 900 Ti Sapphire laser (Coherent Inc.), an argon ion laser at 488nm, and a HeNe laser at 543nm. Images were acquired with a Zeiss Plan-Neofluar 40× 1.3 NA objective. Three-D renderings were created from z-stack acquisitions using Imaris 6.0 software (Bitplane). For EM studies, macrophages were fixed and embedded using standard protocols and sections (600-900 Å) were stained in grids and visualized using a JEOL:-JEM 1200EX II Electron Microscope and a Gatan 782 Digital Camera.

Biochemical Analyses and Enzyme Assays

Enzyme activities were measured with the appropriate fluorimetric or colorimetric substrates (Galjart et al., 1991; Levesque et al., 2001). Cathepsin B and L were assayed using InnoZyme activity assay kits (EMD Biosciences). To measure enzyme activities in the medium, cells were incubated in medium containing 1% BSA (w/v). Protein concentrations were determined using the BCA-assay (Pierce Biotechnology). Uptake of rBV-Neu1 by macrophages was performed as described (Bonten et al., 2004).

Sialic acid containing proteins in mouse BM homogenates were visualized on an SDS-polyacrylamide gel using the ECL-glycoprotein detection system (Pierce Biotechnology) following the manufacturers' protocol.

BMEF was isolated from femurs and tibias of each mouse as described (Levesque et al., 2001).

Macrophage lysates (5 μg) were resolved on reduced 4-12% Bis-Tris SDS-acrylamide gels (Invitrogen) and blotted against PVDF membranes (Millipore), which were subsequently probed with above listed antibodies. Macrophage lysates were N- and O-deglycosylated using the Enzymatic Deglycosylation Kit (Prozyme), following the manufacturers' protocol, and analyzed on Western blots.

Recombinant VCAM-1 (50 ng) or BMSC suspensions were proteolytically digested with 30-μl BMEF (Levesque et al., 2001) and incubated at 37°C for up to 16 hr. Proteolytic fragments were analyzed on Western blots using anti-VCAM-1 antibody.

Metabolic pulse-chase labeling of macrophages with ^{35}S-methionine, immunoprecipitation of radiolabeled proteins with anti-Lamp-1 or anti-Lamp-2 antibodies and autoradiography were performed as described (Proia et al., 1984; Zhou et al., 1996). Band intensity was determined using the Chemidoc system (Bio Rad).

Casein zymograms (Bio Rad) were performed on BMEFs from 2 month-old *Neu1*$^{-/-}$ mice and developed in the presence or absence of selective inhibitors for CG and elastase according to the manufacturer's instructions (EMD Biosciences).

PM proteins were isolated from cultured macrophages and human sialidosis fibroblasts using the Cell Surface Protein Isolation kit (Pierce) and the Qproteome Plasma Membrane Protein Kit (Qiagen), respectively. Lysosomes were purified from fibroblasts as described (Storrie and Madden, 1990). Sialic acid-containing PM proteins were isolated using the Qproteome Glycoprotein Fractionation Kit (Qiagen) and further purified on sialic acid-binding lectin spin columns (MAL). Purified proteins (30 μg) were analyzed on immunblots.

To induce LM-PM fusion of docked lysosomes and extracellular release of their luminal content, cultured cells were incubated for 2 min in medium containing 10 μM Calcimycin A23187 (Sigma) in the presence of 1.2-mM $CaCl_2$, after which the cells were washed with Ca^{2+}-free PBS and further maintained in Ca^{2+}-free medium containing 10-mM EGTA.

Northern Blot Analysis

Total RNA was isolated from 2×10^7 cultured wild-type and *Neu1*$^{-/-}$ macrophages using Trizol (Invitrogen) according to manufacturers' protocol. A Northern blot was prepared with 10-μg RNA per sample and probed with full length ^{32}P-dATP-labeled Lamp-1 cDNA insert, using standard DNA/RNA techniques.

Cell Adhesion Assays, and Analyses of HPCs in the BM and Peripheral Blood

For cell adhesion assays BMSCs were incubated for 1 hr at 37°C with increasing concentrations of KO or WT BMEF, after which calcein-AM-labeled HPCs were added and allowed to adhere for 1 hr. After washing, the retained HPCs were quantified on a TRIAD plate reader (Ex^{485}, Em^{530}; Dynex). Fluorescence readings were standardized against calcein-AM labeled HPCs. Bone marrow and peripheral blood were isolated from 3-month old KO and WT mice (n=4) and stained with lineage-specific antibodies, and c-Kit$^+$/Sca1$^+$/Lin$^-$ HPCs were FACS-sorted. For FACS analyses, cells were incubated for 30 min with fluorochrome-conjugated primary antibodies (0.5-1-μg/1×10^6 cells/50μl). Isotype controls matched the isotypes of the experimental antibodies. Cells were then analyzed on a flow cytometer (FCS LASR II; BD Biosciences).

Two-Dimensional Electrophoresis

BMEF samples from 2-month-old *Neu1*$^{+/+}$ and *Neu1*$^{-/-}$ littermates were TCA-precipitated and resolved in the first dimension on isoelectric focusing gels using broad pH-range ampholytes (pH = 4-10). Reduced proteins were separated in the second dimension on 10% SDS-polyacrylamide gels and stained with SYPRO Ruby (InVitrogen). Gel spots were excised and analyzed by MALDI TOFF mass spectrometry. Proteomic experiments were performed at the Hartwell Center core facility of SJCRH.

Lamp-1 Overexpression in Macrophages

Full-length mouse *Lamp-1* cDNA (IMAGE: 5716524) was subcloned into the mammalian expression vector pIRES2smGFP (http://plasmid.hms.harvard.edu). Macrophages were transiently transfected with either CMV-Lamp-1-IRES-GFP or with CMV-GFP using the Mouse Macrophage Nucleofector electroporation kit and the Nucleofector II electroporation device (Amaxa Biosystems). The average transfection efficiency was 50-60%. GFP-expressing cells were sorted by FACS 24 hr after electroporation, and GFP-positive and negative cells were cultured for an additional 3 days prior to enzyme activity assays.

Silencing of Lamp-1 Expression in Macrophages by siRNA Transfection

WT and Neu1-deficient macrophages were seeded in 6-well dishes at 50% confluency a day before transfection. Cells were transfected with On-Target-plus Smartpool Lamp-1 siRNA (Dharmacon) using Dharmafect-4 transfection reagent. All transfections were performed in

triplicate. Two days after transfection, the medium was replaced with 1-ml serum-free medium plus or minus 10-μM Calcimycin A23187 (Sigma-Aldrich). After 30 min incubation, the medium was collected and assayed for β-hex activity. Cells were analyzed on Western blots or by LSCM.

Supplementary Material

Refer to Web version on PubMed Central for supplementary material.

ACKNOWLEDGEMENTS

We are grateful to Dr. Gerard Grosveld for stimulating discussions and Dr. A. John Harris for critical reading of the manuscript. We thank Dr. Ana Maria Cuervo for the isolation of the lysosomal fractions, Elida Gomero for maintaining the mouse colonies, Fameeka Jenkins and Angela Ingrassia for technical assistance, Linda Mann, and Lingqing Zhang for their help with EM and LSCM imaging, and Vishwajeeth Pagala for the proteomic analyses. A.d'A. holds an endowed chair in Genetics from the Jewelry Charity Fund, and G.Y. was funded in part by an Australian C.J. Martin fellowship. This work was supported in part by the NIH grants GM60905 and DK52025, the Assisi Foundation of Memphis and the American Syrian Associated Charities (ALSAC) of SJCRH.

REFERENCES

Andrejewski N, Punnonen EL, Guhde G, Tanaka Y, Lullmann-Rauch R, Hartmann D, von Figura K, Saftig P. Normal lysosomal morphology and function in LAMP-1-deficient mice. J Biol Chem 1999;274:12692–12701. [PubMed: 10212251]

Andrews NW. Regulated secretion of conventional lysosomes. Trends Cell Biol 2000;10:316–321. [PubMed: 10884683]

Andrews NW, Chakrabarti S. There's more to life than neurotransmission: the regulation of exocytosis by synaptotagmin VII. Trends Cell Biol 2005;15:626–631. [PubMed: 16168654]

Axelrod D. Cell-substrate contacts illuminated by total internal reflection fluorescence. J Cell Biol 1981;89:141–145. [PubMed: 7014571]

Bonten E, Spoel A. v. d. Fornerod M, Grosveld G, d'Azzo A. Characterization of human lysosomal neuraminidase defines the molecular basis of the metabolic storage disorder sialidosis. Genes Dev 1996;10:3156–3169. [PubMed: 8985184]

Bonten EJ, Arts WF, Beck M, Covanis A, Donati MA, Parini R, Zammarchi E, d'Azzo A. Novel mutations in lysosomal neuraminidase identify functional domains and determine clinical severity in sialidosis. Hum Mol Genet 2000;9:2715–2725. [PubMed: 11063730]

Bonten EJ, Wang D, Toy JN, Mann L, Mignardot A, Yogalingam G, d'Azzo A. Targeting macrophages with baculovirus-produced lysosomal enzymes: implications for enzyme replacement therapy of the glycoprotein storage disorder galactosialidosis. FASEB J 2004;9:971–973. [PubMed: 15084520]

Borriello F, Krauter KS. Multiple murine alpha 1-protease inhibitor genes show unusual evolutionary divergence. Proc Natl Acad Sci U S A 1991;88:9417–9421. [PubMed: 1946354]

Bossi G, Booth S, Clark R, Davis EG, Liesner R, Richards K, Starcevic M, Stinchcombe J, Trambas C, Dell'Angelica EC, Griffiths GM. Normal lytic granule secretion by cytotoxic T lymphocytes deficient in BLOC-1, -2 and -3 and myosins Va, VIIa and XV. Traffic 2005;6:243–251. [PubMed: 15702992]

Bossi G, Griffiths GM. CTL secretory lysosomes: biogenesis and secretion of a harmful organelle. Semin Immunol 2005;17:87–94. [PubMed: 15582491]

Chakrabarti S, Kobayashi KS, Flavell RA, Marks CB, Miyake K, Liston DR, Fowler KT, Gorelick FS, Andrews NW. Impaired membrane resealing and autoimmune myositis in synaptotagmin VII-deficient mice. J Cell Biol 2003;162:543–549. [PubMed: 12925704]

Cuervo AM, Mann L, Bonten EJ, d'Azzo A, Dice JF. Cathepsin A regulates chaperone-mediated autophagy through cleavage of the lysosomal receptor. EMBO J 2003;22:47–59. [PubMed: 12505983]

Dahlgren C, Carlsson S, Karlsson A, Lundqvist H, Sjölin C. The lysosomal membrane glycoproteins Lamp-1 and Lamp-2 are present in mobilizable organelles, but are absent from the azurophil granules of human neutrophils. Biochem J 1995;311:667–674. [PubMed: 7487911]

de Geest N, Bonten E, Mann L, de Sousa-Hitzler J, Hahn C, d'Azzo A. Systemic and neurologic abnormalities distinguish the lysosomal disorders sialidosis and galactosialidosis in mice. Hum Mol Genet 2002;11:1455–1464. [PubMed: 12023988]

Eskelinen EL, Tanaka Y, Saftig P. At the acidic edge: emerging functions for lysosomal membrane proteins. Trends Cell Biol 2003;13:137–145. [PubMed: 12628346]

Forsyth S, Horvath A, Coughlin P. A review and comparison of the murine alpha1-antitrypsin and alpha1-antichymotrypsin multigene clusters with the human clade A serpins. Genomics 2003;81:336–345. [PubMed: 12659817]

Furuno K, Ishikawa T, Akasaki K, Yano S, Tanaka Y, Yamaguchi Y, Tsuji H, Himeno M, Kato K. Morphological localization of a major lysosomal membrane glycoprotein in the endocytic membrane system. J Biochem (Tokyo) 1989;106:708–716. [PubMed: 2691512]

Galjart NJ, Morreau H, Willemsen R, Gillemans N, Bonten EJ, d'Azzo A. Human lysosomal protective protein has cathepsin A-like activity distinct from its protective function. J Biol Chem 1991;266:14754–14762. [PubMed: 1907282]

Gerasimenko JV, Gerasimenko OV, Petersen OH. Membrane repair: Ca(2+)-elicited lysosomal exocytosis. Curr Biol 2001;11(R97):91–94.

Hahn C, Martin M, Schröder M, Vanier M, Hara Y, Suzuki K, Suzuki K, d'Azzo A. Generalized CNS disease and massive Gm1-ganglioside accumulation in mice defective in lysosomal acid ß-galactosidase. Hum Mol Gen 1997;6:205–211. [PubMed: 9063740]

Huynh C, Roth D, Ward DM, Kaplan J, Andrews NW. Defective lysosomal exocytosis and plasma membrane repair in Chediak-Higashi/beige cells. Proc Natl Acad Sci U S A 2004;101:16795–16800. [PubMed: 15557559]

Huynh KK, Eskelinen EL, Scott CC, Malevanets A, Saftig P, Grinstein S. LAMP proteins are required for fusion of lysosomes with phagosomes. EMBO J 2007;26:313–324. [PubMed: 17245426]

Jaiswal JK, Andrews NW, Simon SM. Membrane proximal lysosomes are the major vesicles responsible for calcium-dependent exocytosis in nonsecretory cells. J Cell Biol 2002;159:625–635. [PubMed: 12438417]

Kima PE, Burleigh B, Andrews NW. Surface-targeted lysosomal membrane glycoprotein-1 (Lamp-1) enhances lysosome exocytosis and cell invasion by Trypanosoma cruzi. Cell Microbiol 2000;2:477–486. [PubMed: 11207602]

Kominami E, Tsukahara T, Hara K, Katunuma N. Biosyntheses and processing of lysosomal cysteine proteinases in rat macrophages. FEBS Lett 1988;231:225–228. [PubMed: 3360126]

Kornfeld S, Mellman I. The biogenesis of lysosomes. Annu Rev Cell Biol 1989;5:483–525. [PubMed: 2557062]

Kundra R, Kornfeld S. Asparagine-linked oligosaccharides protect Lamp-1 and Lamp-2 from intracellular proteolysis. J Biol Chem 1999;274:31039–31046. [PubMed: 10521503]

Levesque JP, Takamatsu Y, Nilsson SK, Haylock DN, Simmons PJ. Vascular cell adhesion molecule-1 (CD106) is cleaved by neutrophil proteases in the bone marrow following hematopoietic progenitor cell mobilization by granulocyte colony-stimulating factor. Blood 2001;98:1289–1297. [PubMed: 11520773]

Li P, Gregg JL, Wang N, Zhou D, O'Donnell P, Blum JS, Crotzer VL. Compartmentalization of class II antigen presentation: contribution of cytoplasmic and endosomal processing. Immunol Rev 2005;207:206–217. [PubMed: 16181338]

Lippincott-Schwartz J, Fambrough DM. Cycling of the integral membrane glycoprotein, LEP100, between plasma membrane and lysosomes: kinetic and morphological analysis. Cell 1987;49:669–677. [PubMed: 3107839]

Martinez I, Chakrabarti S, Hellevik T, Morehead J, Fowler K, Andrews NW. Synaptotagmin VII regulates Ca(2+)-dependent exocytosis of lysosomes in fibroblasts. J Cell Biol 2000;148:1141–1149. [PubMed: 10725327]

McNeil PL, Steinhardt RA. Plasma membrane disruption: repair, prevention, adaptation. Annu Rev Cell Dev Biol 2003;19:697–731. [PubMed: 14570587]

Ni X, Canuel M, Morales CR. The sorting and trafficking of lysosomal proteins. Histol Histopathol 2006;21:899–913. [PubMed: 16691542]

Oakes SA, Scorrano L, Opferman JT, Bassik MC, Nishino M, Pozzan T, Korsmeyer SJ. Proapoptotic BAX and BAK regulate the type 1 inositol trisphosphate receptor and calcium leak from the endoplasmic reticulum. Proc Natl Acad Sci U S A 2005;102:105–110. [PubMed: 15613488]

Patston PA, Church FC, Olson ST. Serpin-ligand interactions. Methods 2004;32:93–109. [PubMed: 14698622]

Proia RL, d'Azzo A, Neufeld EF. Association of alpha- and beta-subunits during the biosynthesis of beta-hexosaminidase in cultured human fibroblasts. J Biol Chem 1984;259:3350–3354. [PubMed: 6230359]

Reddy A, Caler EV, Andrews NW. Plasma membrane repair is mediated by Ca(2+)-regulated exocytosis of lysosomes. Cell 2001;106:157–169. [PubMed: 11511344]

Rizo J, Chen X, Arac D. Unraveling the mechanisms of synaptotagmin and SNARE function in neurotransmitter release. Trends Cell Biol 2006;7:339–350. [PubMed: 16698267]

Rottier R, Bonten E, d'Azzo A. A point mutation in the *neu-1* locus causes the neuraminidase defect in the SM/J mouse. Hum Mol Genet 1998;7:313–321. [PubMed: 9425240]

Roy D, Liston DR, Idone VJ, Di A, Nelson DJ, Pujol C, Bliska JB, Chakrabarti S, Andrews NW. A process for controlling intracellular bacterial infections induced by membrane injury. Science 2004;304:1515–1518. [PubMed: 15178804]

Sandhoff, K.; Kolter, T.; Harzer, K.; Hirschhorn, R.; Reuser, A.; Neufeld, EF.; Muenzer, J.; Gelb, BD.; Bromme, D.; Desnick, RJ., et al. Lysosomal disorders. In: Scriver, CR.; Beaudet, L.; Sly, WS.; Valle, D., editors. The metabolic and molecular bases of inherited disease. McGraw-Hill; New York: 2001. p. 3371-3894.

Seto ES, Bellen HJ, Lloyd TE. When cell biology meets development: endocytic regulation of signaling pathways. Genes Dev 2002;16:1314–1336. [PubMed: 12050111]

Shen SS, Tucker WC, Chapman ER, Steinhardt RA. Molecular regulation of membrane resealing in 3T3 fibroblasts. J Biol Chem 2005;280:1652–1660. [PubMed: 15536080]

Sklar MD, Tereba A, Chen BD, Walker WS. Transformation of mouse bone marrow cells by transfection with a human oncogene related to c-myc is associated with the endogenous production of macrophage colony stimulating factor 1. J Cell Physiol 1985;125:403–412. [PubMed: 3877730]

Stinchcombe J, Bossi G, Griffiths GM. Linking albinism and immunity: the secrets of secretory lysosomes. Science 2004;305:55–59. [PubMed: 15232098]

Storrie B, Madden EA. Isolation of subcellular organelles. Methods Enzymol 1990;182:203–225. [PubMed: 2156127]

Tanaka Y, Guhde G, Suter A, Eskelinen EL, Hartmann D, Lullmann-Rauch R, Janssen PM, Blanz J, von Figura K, Saftig P. Accumulation of autophagic vacuoles and cardiomyopathy in LAMP-2-deficient mice. Nature 2000;406:902–906. [PubMed: 10972293]

Thomas, GH. Disorders of glycoprotein degradation and structure: alpha-mannosidosis, beta-mannosidosis, fucosidosis, and sialidosis. In: Scriver, CR.; Beaudet, AL.; Sly, WS.; Valle, D., editors. The Metabolic and Molecular Bases of Inherited Disease. McGraw Hill, Inc.; New York: 2001. p. 3507-3534.

Tucker WC, Weber T, Chapman ER. Reconstitution of Ca2+- regulated membrane fusion by synaptotagmin and SNAREs. Science 2004;304:435–438. [PubMed: 15044754]

Winkler IG, Hendy J, Coughlin P, Horvath A, Levesque JP. Serine protease inhibitors serpina1 and serpina3 are down-regulated in bone marrow during hematopoietic progenitor mobilization. J Exp Med 2005;201:1077–1088. [PubMed: 15795238]

Zhou X-Y, van der Spoel A, Rottier R, Hale G, Willemsen R, Berry GT, Strisciuglio P, Andria G, d'Azzo A. Molecular and biochemical analysis of protective protein/cathepsin A mutations: Correlation with clinical severity in galactosialidosis. Hum Mol Genet 1996;5:1977–1987. [PubMed: 8968752]

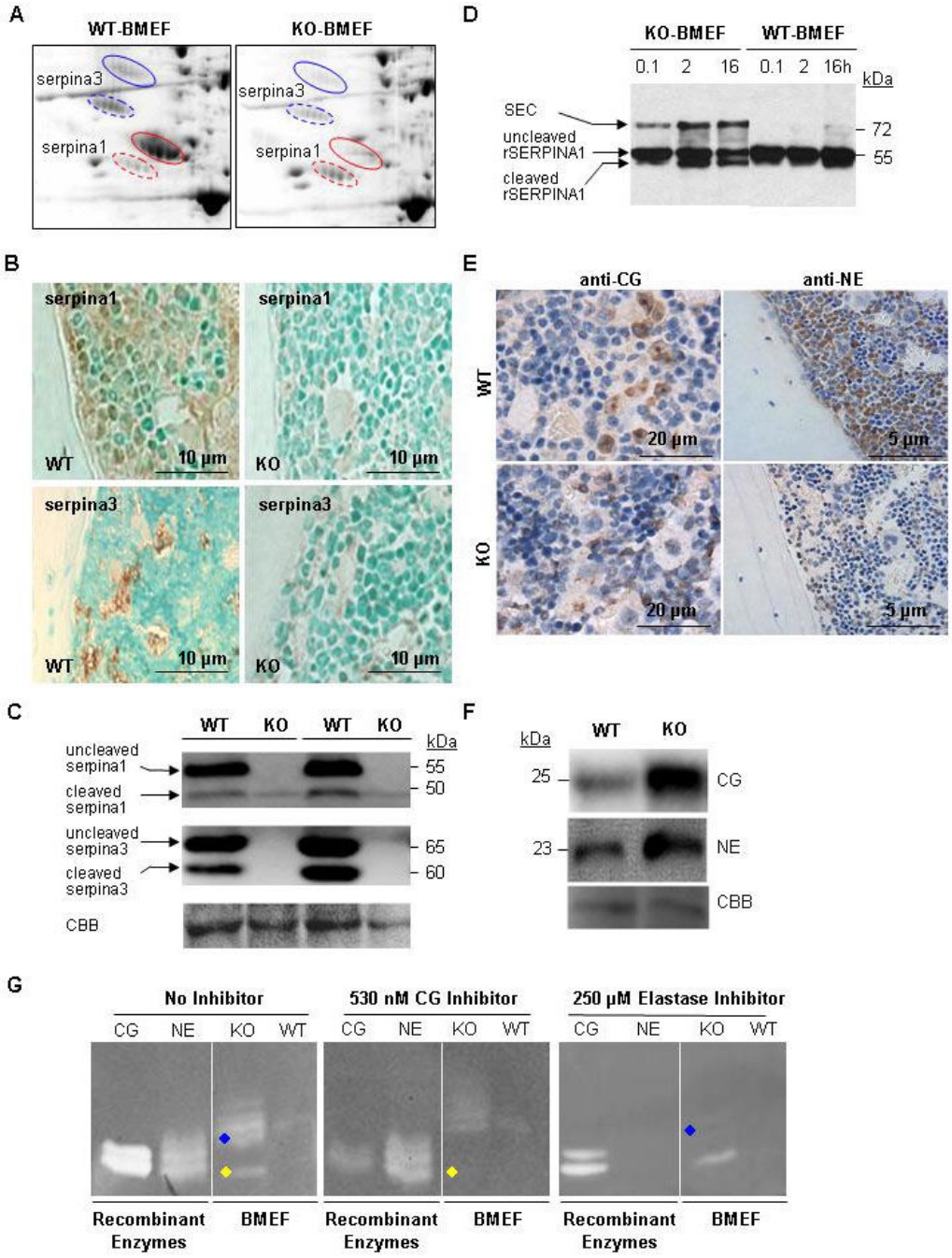

Figure 1. Serpins are Downregulated in the *Neu1*$^{-/-}$ Bone Niche by Increased Exocytosis of Neutrophil Serine Proteases

(A) 2D-electrophoresis of BMEFs from KO and WT littermates; uncleaved serpina3 (blue circles) and serpina1 (red circles); cleaved serpina1 and serpina3 (dashed circles).

(B) Bone tissue sections probed with anti-serpina1 and anti-serpina3.

(C) Immunoblots of WT and KO BMEF probed with serpina1 and serpina3 antibodies. Coomassie brilliant blue (CBB) staining showed equal loading.

(D) immunoblots of recombinant SERPINA1 after incubation with KO and WT BMEF.

(E) Immunostaining of KO bone sections with anti-CG and anti-NE antibodies.

(F) immunoblots of WT and KO BMEF with anti-CG and andti-NE antibodies.

(G) Casein zymography of WT and KO BMEF in the presence and absence of CG and elastase inhibitors. Serine protease inhibited by the CG inhibitor (yellow diamond, middle panel); high MW serine protease inhibited by the elastase inhibitor (blue diamond, right panel).

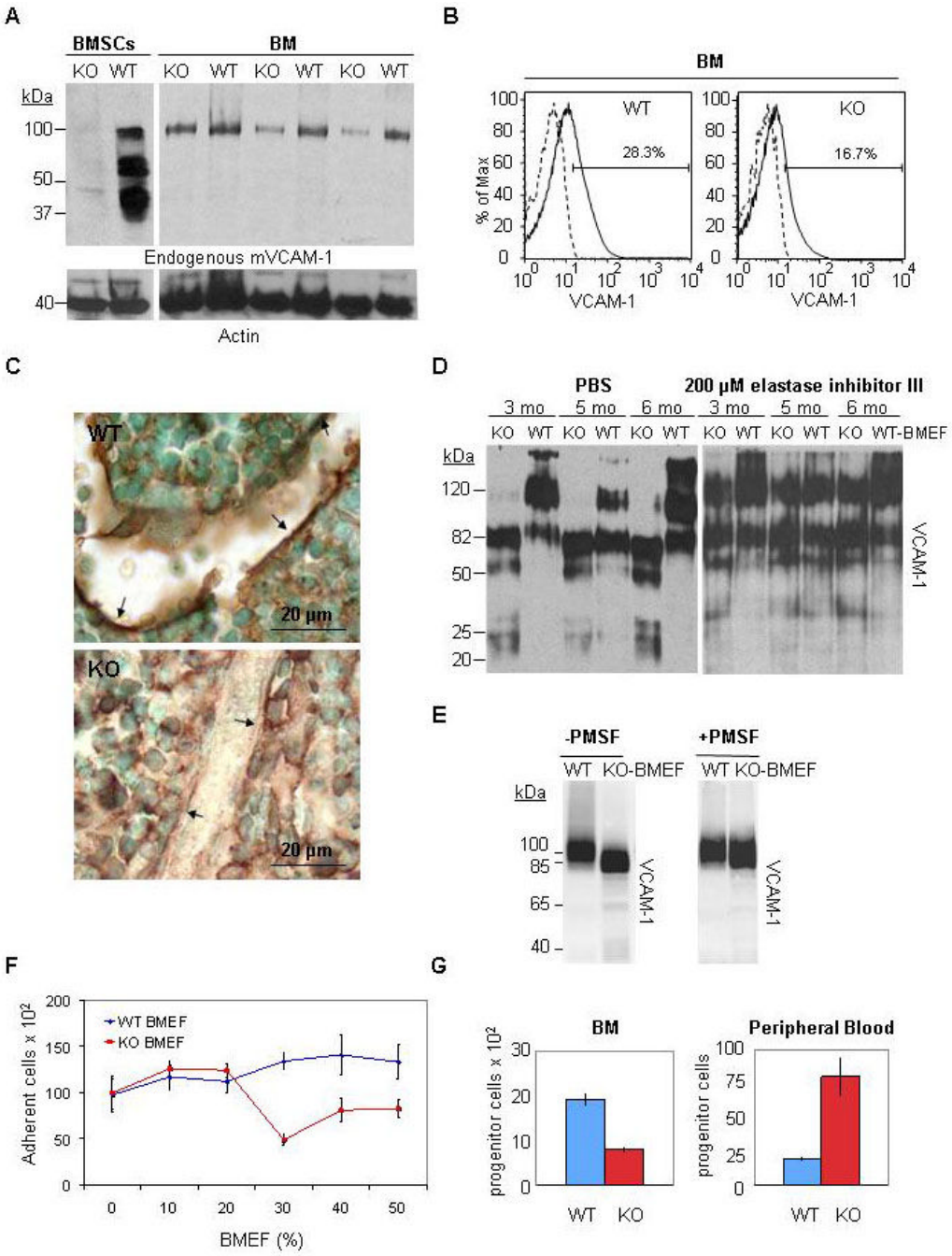

Figure 2. Elevated Elastase-like Activity in *Neu1*$^{-/-}$ BMEF Proteolytically Degrades VCAM-1

(A) Immunoblots of BMSC and BM lysates from WT and KO mouse littermate pairs of different ages (1, 3, 5 months, respectively) probed with anti-VCAM-1 antibody.

(B) FACS profiles of KO BM obtained with FITC-conjugated VCAM-1 antibody. Dotted graphs represent IgG isotype controls set at zero percent.

(C) Bone sections from 2-month-old KO and WT mice stained with anti-VCAM-1; strong immunoreactivity only in WT sections in the region lining the bone (arrows).

(D) Aliquots of rhVCAM-1 were incubated with BMEF from WT and KO mice in the presence or absence (PBS) of an elastase inhibitor and analyzed on immunoblots probed with anti-VCAM-1 antibody.

(E) Incubation of WT BMSCs with KO BMEF in presence or absence of serine protease inhibitor PMSF, followed by immunoblot analysis using anti-VCAM-1 antibody.
(F) WT BMSCs were incubated with increasing concentrations of WT or KO BMEF, followed by addition to the culture of fluorescently labeled WT BM-derived HPCs. Retained HPCs were quantified by measuring the fluorescence. Values are presented as mean ± SEM.
(G) FACS analysis of c-Kit^{+}/Sca1^{+}/Lin^{-} HPCs; age of mice, 4 months; n=4; values represent the mean ± SEM.

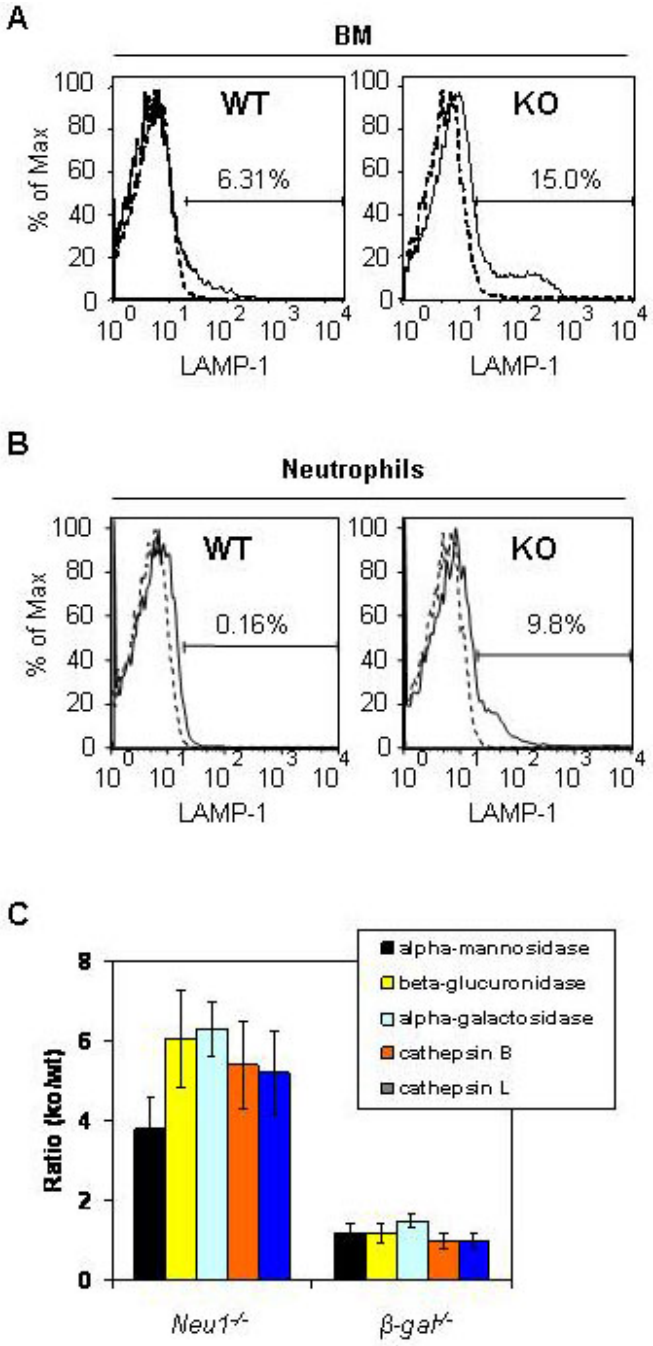

Figure 3. Lysosomal Exocytosis is Increased in the *Neu1*$^{-/-}$ Bone Niche

(A) FACS analysis of total BM cells from 3-month old WT and KO littermates with FITC-conjugated anti-Lamp-1 (1D4B).

(B) FACS analysis of gated Mac1^{+}/Gr1^{+} BM neutrophils. Dotted graphs represent IgG isotype controls set at zero percent.

(C) Lysosomal glycosidase and cathepsin activities were measured in BMEFs from WT, *Neu1*$^{-/-}$ and *β-gal*$^{-/-}$ mice. Activities are expressed as ratios of KO and WT values. Values represent the mean ± SD (n=5 mice).

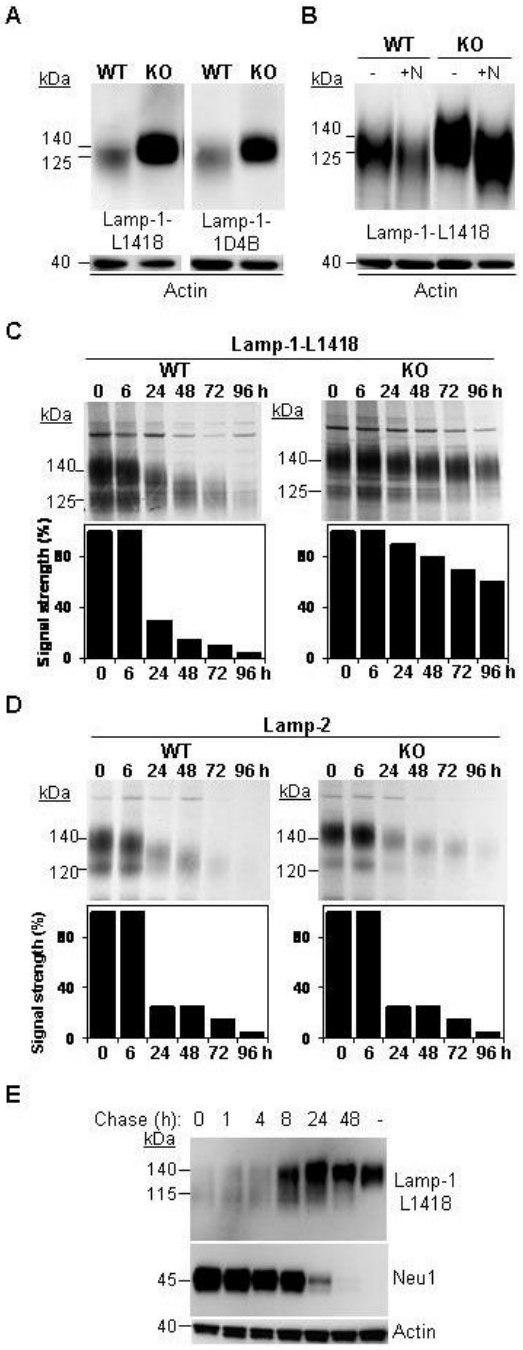

Figure 4. Lamp-1 is a Substrate of Neu1

(A) WT and KO macrophage lysates were analyzed on immunoblots probed with anti-Lamp1 antibodies; L1418 recognizes the C-terminal peptide; 1D4B recognizes the luminal domain.

(B) Immunoblot analysis of WT and KO macrophages with anti-Lamp1 antibody after uptake of rBV-Neu1 (+N).

(C and D) Pulse-chase analyses of radiolabeled Lamp-1 and Lamp-2 in KO and WT macrophages.

(E) Immunoblot of KO macrophages probed with Lamp-1 and Neu-1 antibodies; macrophages were incubated with rBV-Neu and chased for different time periods in Neu1-free medium. Actin was used as a loading control.

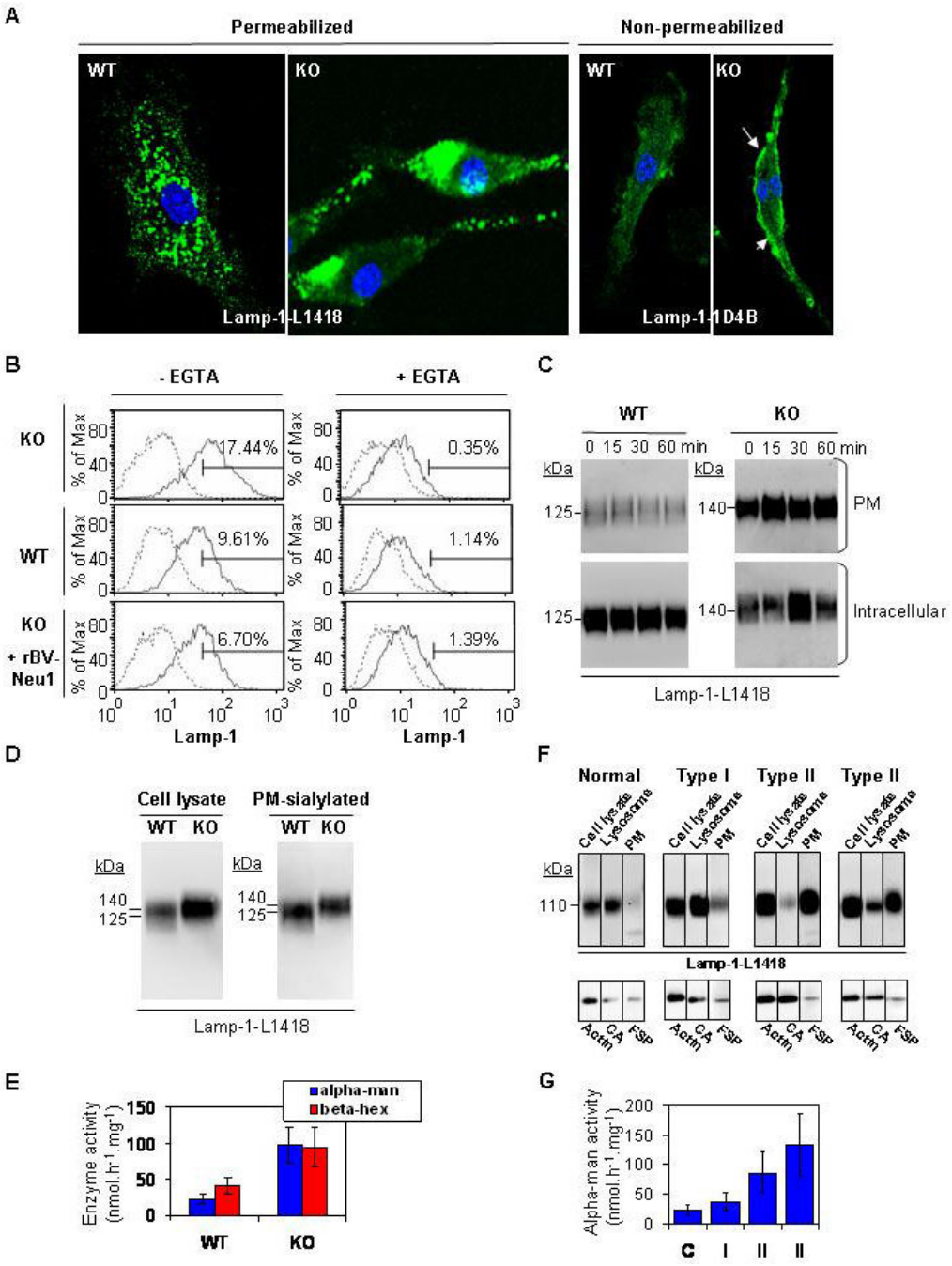

Figure 5. Enhanced Lysosomal Exocytosis in *Neu1*$^{-/-}$ Macrophages and Type II Sialidosis Fibroblasts and Increased Levels of LAMP-1 at the Cell Surface

(A) Comparison of immunofluoresence staining of permeabilized and non-permeabilized WT or KO macrophages with Lamp-1 antibodies (L1418 or 1D4B), followed by LSCM; PM distribution of Lamp-1 (arrows) in non-permeabilized KO macrophages. Magnification, 100x. (B) WT and KO macrophages were cultured in the presence or absence of rBV-Neu1, as indicated. Cell surface expression of Lamp-1 was detected by FACS, using anti-Lamp-1 (1D4B). Prior to the FACS analysis, cultures were incubated in either normal medium (-EGTA) or in Ca^{2+}-depleted medium (+EGTA). Dotted graphs represent IgG isotype controls set at zero percent.

(C) Immunoblots of PM and intracellular fractions isolated from WT and KO macrophages after treatment with calcimycin, followed by culture of the cells in Ca^{2+}-free medium for different time points (0, 15, 30, 60 min).
(D) PM preparations from WT and KO macrophages were purified with a sialic acid-specific lectin and analyzed on immunoblots with anti-Lamp-1 (L1418). Cell lysates were included as controls.
(E) Increased β-hex and α-man activities in the medium of KO cells compared to WT. Enzyme activities represent the mean ± SEM.
(F) PM and lysosomal preparations purified from normal fibroblasts, type I (mild) and type II (severe) sialidosis fibroblasts were analyzed on immunoblots with anti-Lamp-1 (L1418). Total cell lysates were used as controls. For equal loading, membranes were incubated with anti-actin (cell lysates), anti-CA (lysosomes), and anti-fibroblast surface protein (FSP; PM).
(G) Increased α-man activity was measured in the medium of type II sialidosis fibroblasts. Enzyme activities represent the mean ± SEM.

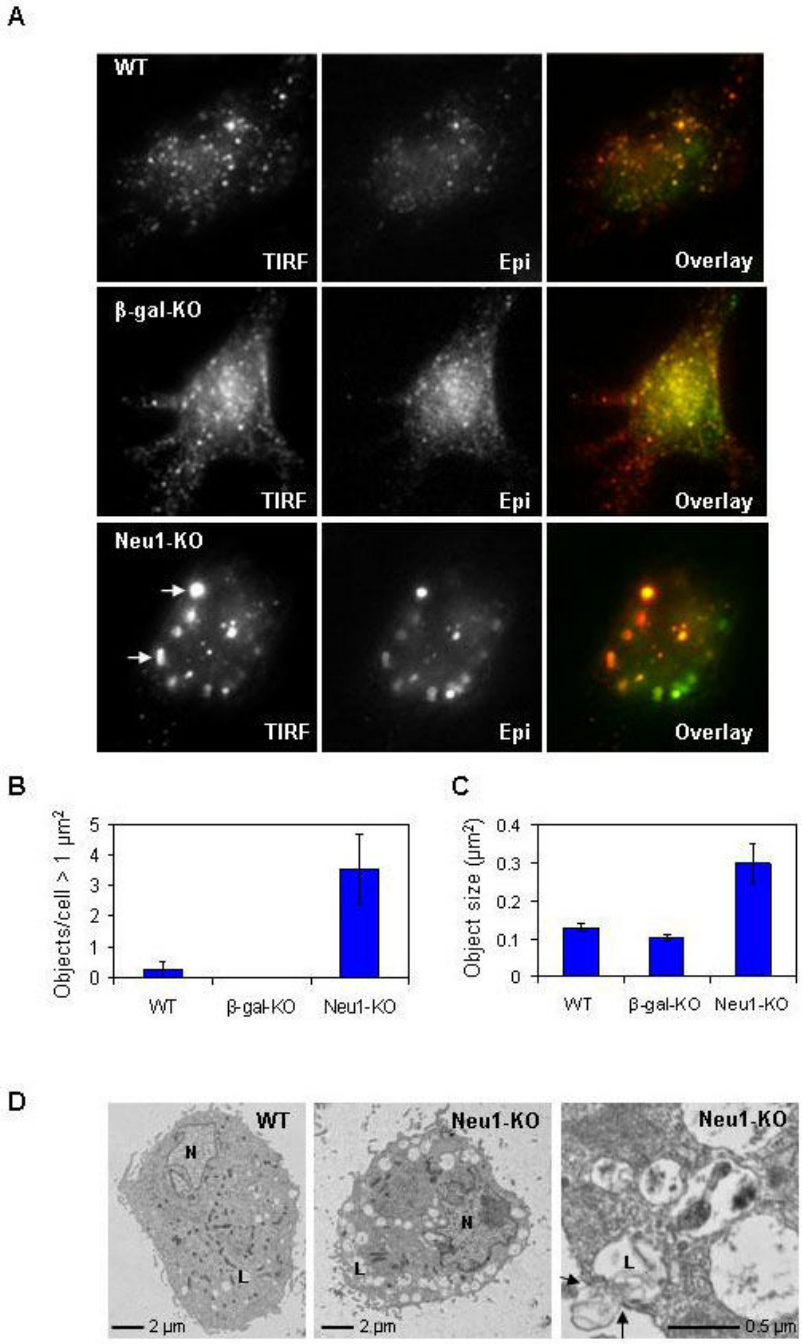

Figure 6. *Neu1*$^{-/-}$ Macrophages Have 'Clusters' of PM-Proximal Lysosomes

WT, *β-gal*$^{-/-}$ (β-gal-KO), and *Neu1*$^{-/-}$ (Neu1-KO) macrophages were incubated for 30 min with Lysotracker. The cells were analyzed by TIRFM to determine the number of lysosomes in the evanescent field proximal to the PM.

(A) Representative images of evanescent (TIRF; red in overlay) and epifluorescent (Epi; green in overlay) lysotracker^{+} cells; multiple large (>1μm) 'clusters' (arrows) in the evanescent field of Neu1-KO cells. Magnification, 60x.

(B) Lysotracker^{+} objects larger than 1-μm were counted in multiple images of each cell-type (n=20). The values represent mean objects per cell +/- SD.

(C) The mean size of lysotracker+ objects was calculated for each of the 3 cell-types (n=20). The values represent mean object size +/- SD.
(D) EM of WT and KO macrophages; lysosome that has breached the PM and is being exocytosed (arrows).

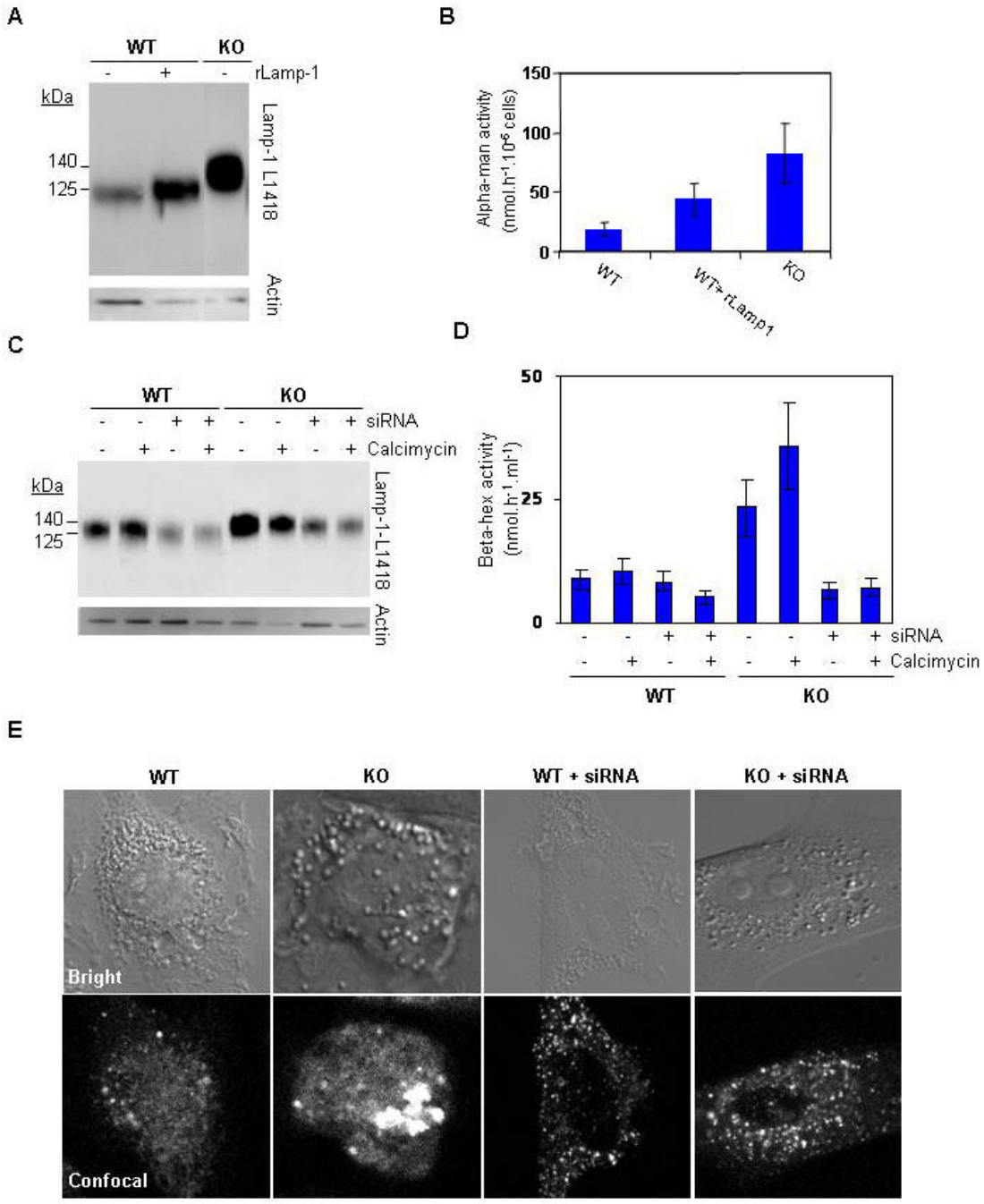

Figure 7. Lamp-1 Regulates the Level of Lysosomal Exocytosis and Promotes the Formation of Lysosome Clusters in *Neu1*$^{-/-}$ Cells

(A) CMV-Lamp-1-IRES-GFP plasmid DNA was transfected into WT macrophages, and Lamp-1 expression was analyzed on immunoblot with anti-Lamp-1; Lamp-1/GFP overexpressing cells (WT, +); CMV-GFP transfected cells (WT, -); mock-transfected KO cells (KO, -).

(B) WT and KO macrophages were transiently transfected with either CMV-GFP or CMV-Lamp-1-GFP and FACS-sorted. Alpha-man activity was measured in the medium of GFP^{+}/rLamp-1^{+} WT (WT+rLamp1) and GFP^{-}/rLamp-1^{-} WT cells (WT). Enzyme activities are expressed as the mean ± SEM.

(C) WT and KO macrophages were transfected with Lamp-1 siRNA or mock-transfected, in presence or absence of calcimycin. Cell lysates were analyzed on an immunoblot probed with anti-Lamp1 antibody.
(D) Beta-hex activity measured in the medium of mock or Lamp-1-siRNA-transfected WT and KO macrophages, in the presence or absence of calcimycin. Enzyme activities are expressed as mean ± SEM.
(E) WT and KO macrophages were either mock- or Lamp-1-siRNA transfected. After transfection the cells were incubated with Lysotracker and analyzed by LSCM. Magnification, 60x.

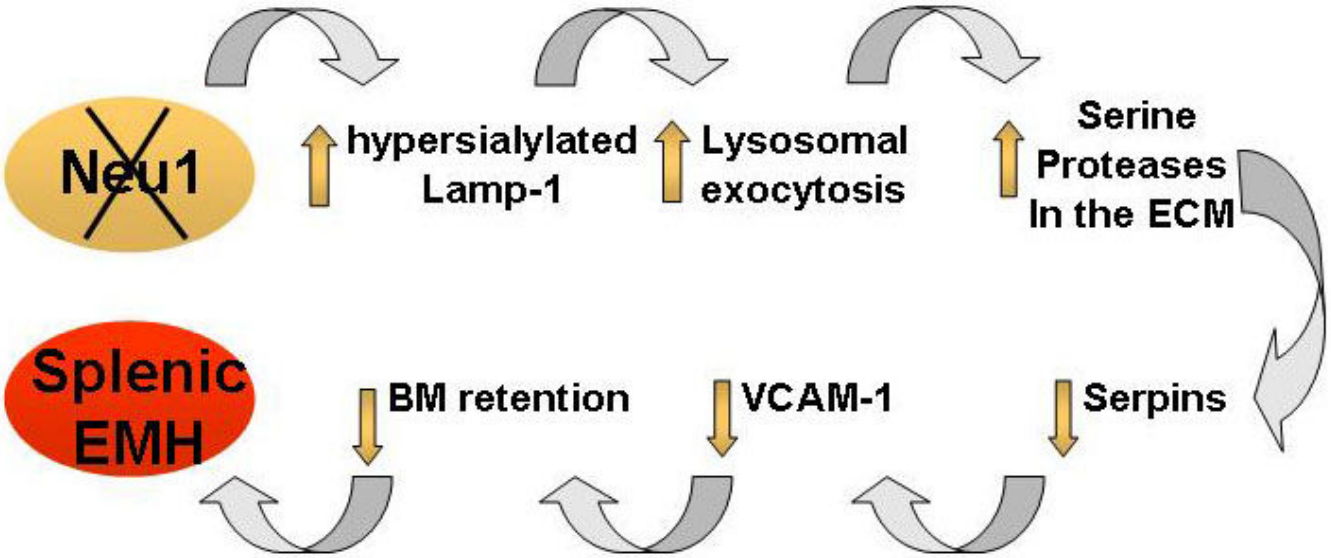

Figure 8. Schematic Representation of the Events that Lead to Loss of BM and Splenic EMH in Neu1-Deficient Mice